Binary Black Hole Population Properties Inferred from the First and Second Observing Runs of Advanced LIGO and Advanced Virgo

Tomofumi Shimoda

Ando lab seminar on Dec. 7

Paper

- arXiv:1811.12940

DRAFT VERSION NOVEMBER 29, 2018
Typeset using LaTeX **twocolumn** style in AASTeX62

Binary Black Hole Population Properties Inferred from the First and Second Observing Runs of Advanced LIGO and Advanced Virgo

THE LIGO SCIENTIFIC COLLABORATION AND THE VIRGO COLLABORATION

ABSTRACT

We present results on the mass, spin, and redshift distributions of the ten binary black hole mergers detected in Advanced LIGO's and Advanced Virgo's first and second observing runs. We constrain properties of the binary black hole (BBH) mass spectrum using models with a range of parameterizations of the BBH mass and spin distributions. We find that the mass distribution of the more massive black hole in each binary is well approximated by models with almost no black holes larger than 45 $M_{\odot}$, and a power law index of $\alpha = 1.6^{+1.5}_{-1.7}$ (90% credibility). We also show that BBHs are unlikely to be composed of black holes with large spins aligned to the orbital angular momentum. Modelling the evolution of the BBH merger rate with redshift, we show that it is increasing with redshift with credibility 0.88. Marginalizing over uncertainties in the BBH population, we find robust estimates of the BBH merger rate density of $R = 52.9^{+55.6}_{-27.0}\ \mathrm{Gpc}^{-3}\ \mathrm{yr}^{-1}$(90% credibility). As the BBH catalog grows in future observing runs, we expect that uncertainties in the population model parameters will shrink, potentially providing insights into the formation of black holes via supernovae, binary interactions of massive stars, stellar cluster dynamics, and the formation history of black holes across cosmic time.

Paper2

- arXiv:1811.12907

GWTC-1: A Gravitational-Wave Transient Catalog of Compact Binary Mergers Observed by LIGO and Virgo during the First and Second Observing Runs

The LIGO Scientific Collaboration and The Virgo Collaboration

(Compiled: 30 November 2018)

We present the results from three gravitational-wave searches for coalescing compact binaries with component masses above $1M_\odot$ during the first and second observing runs of the Advanced gravitational-wave detector network. During the first observing run (O1), from September 12th, 2015 to January 19th, 2016, gravitational waves from three binary black hole mergers were detected. The second observing run (O2), which ran from November 30th, 2016 to August 25th, 2017, saw the first detection of gravitational waves from a binary neutron star inspiral, in addition to the observation of gravitational waves from a total of seven binary black hole mergers, four of which we report here for the first time: GW170729, GW170809, GW170818 and GW170823. For all significant gravitational-wave events, we provide estimates of the source properties. The detected binary black holes have total masses between $18.6^{+3.1}_{-0.7}M_\odot$ and $85.1^{+15.6}_{-10.9}M_\odot$, and range in distance between 320^{+120}_{-110} Mpc and 2750^{+1350}_{-1320} Mpc. No neutron star – black hole mergers were detected. In addition to highly significant gravitational-wave events, we also provide a list of marginal event candidates with an estimated false alarm rate less than 1 per 30 days. From these results over the first two observing runs, which include approximately one gravitational-wave detection per 15 days of data searched, we infer merger rates at the 90% confidence intervals of $110-3840\ \mathrm{Gpc}^{-3}\ \mathrm{y}^{-1}$ for binary neutron stars and $9.7-101\ \mathrm{Gpc}^{-3}\ \mathrm{y}^{-1}$ for binary black holes, and determine a neutron star – black hole merger rate 90% upper limit of $610\ \mathrm{Gpc}^{-3}\ \mathrm{y}^{-1}$.

PACS numbers: 04.80.Nn, 04.25.dg, 95.85.Sz, 97.80.-d 04.30.Db, 04.30.Tv

I. INTRODUCTION

use waveform models to compare against the data, but instead identifies regions of excess power in the time-frequency rep-

Abstract

- LIGO & Virgo have reported the detection of 10 BBHs (+1 BNS) during O1 and O2
  - 6 already reported BBHs + <u>4 new BBHs</u>

- Based on the parameters of the detected BBHs, better or new constrains on the population properties of BBHs have been inferred

- BBH population will provide information on the formation process and surrounding environments

Observation runs

LLO
BNS : 69 Mpc
BBH : 845 Mpc

LHO
BNS : 76 Mpc
BBH : 931 Mpc

LLO
BNS : 84 Mpc
BBH : 1029 Mpc

LHO
BNS : 68 Mpc
BBH : 831 Mpc

Virgo
BNS : 26 Mpc
BBH : ?

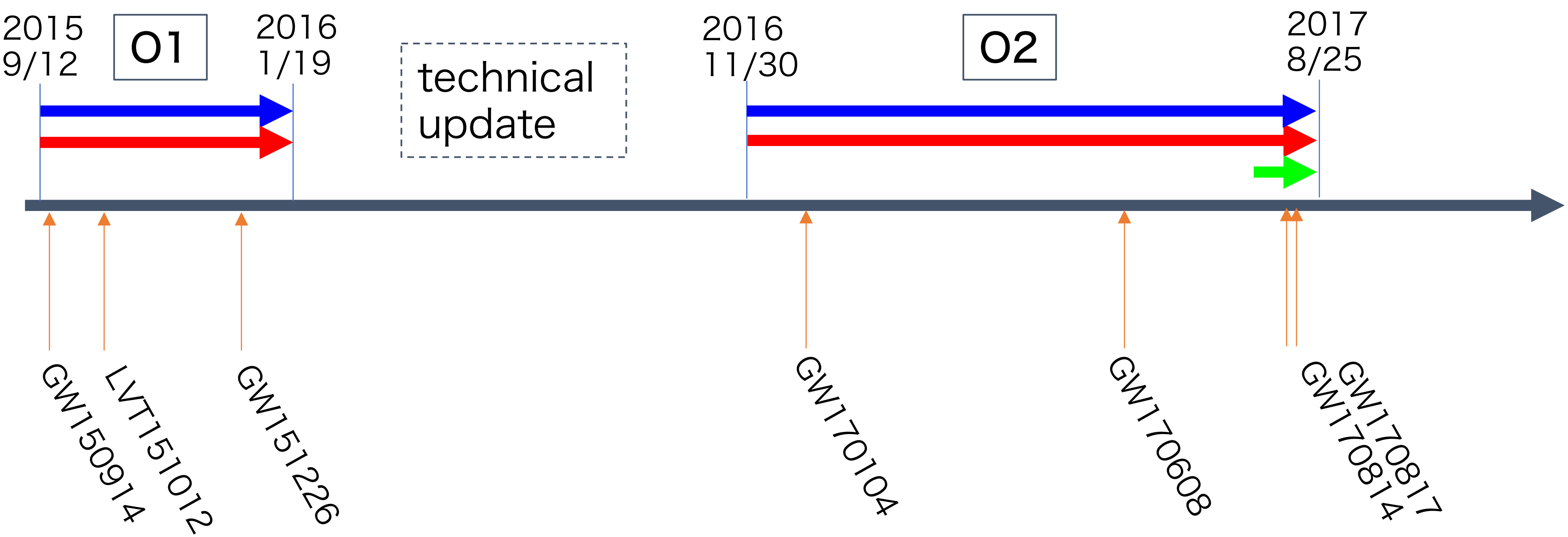

Newly reported binaries

LLO
BNS : 69 Mpc
BBH : 845 Mpc

LHO
BNS : 76 Mpc
BBH : 931 Mpc

LLO
BNS : 84 Mpc
BBH : 1029 Mpc

LHO
BNS : 68 Mpc
BBH : 831 Mpc

Virgo
BNS : 26 Mpc
BBH : ?

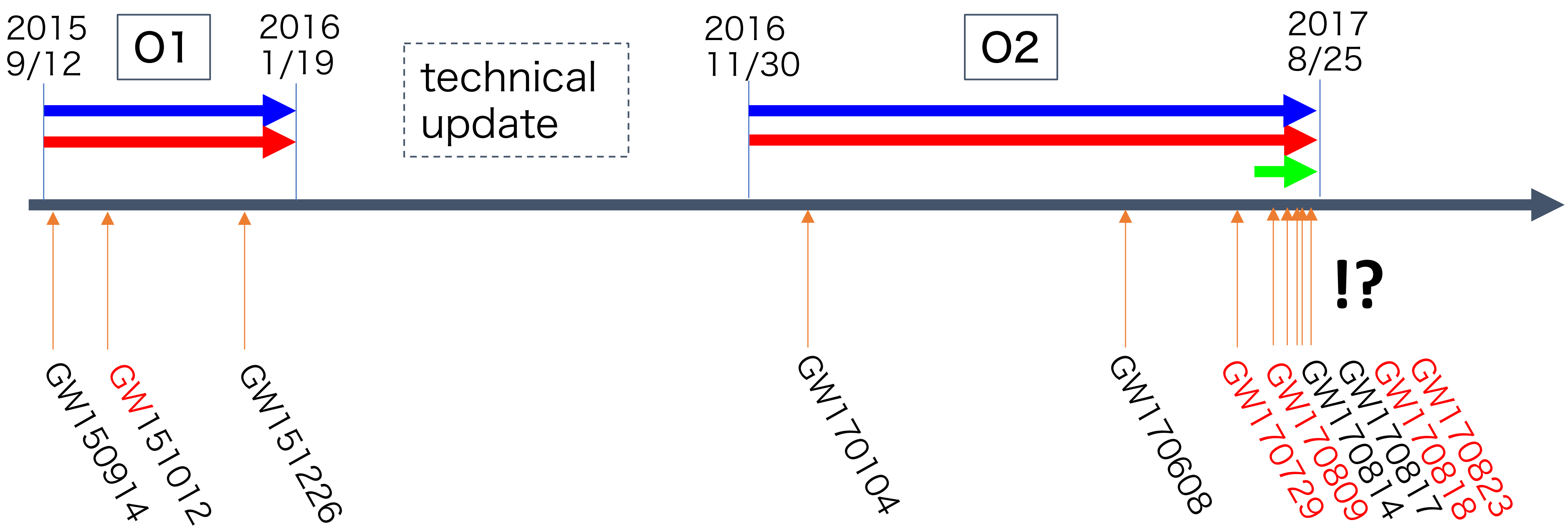

10 BBHs & 1 BNS

Parameters of BBHs

Event	$m_1/\mathrm{M}_\odot$	$m_2/\mathrm{M}_\odot$	$\mathcal{M}/\mathrm{M}_\odot$	χ_{eff}	$M_{\mathrm{f}}/\mathrm{M}_\odot$	a_{f}	$E_{\mathrm{rad}}/(\mathrm{M}_\odot c^2)$	$\ell_{\mathrm{peak}}/(\mathrm{erg\,s}^{-1})$	d_L/Mpc	z	$\Delta\Omega/\mathrm{deg}^2$
GW150914	$35.6^{+4.8}_{-3.0}$	$30.6^{+3.0}_{-4.4}$	$28.6^{+1.6}_{-1.5}$	$-0.01^{+0.12}_{-0.13}$	$63.1^{+3.3}_{-3.0}$	$0.69^{+0.05}_{-0.04}$	$3.1^{+0.4}_{-0.4}$	$3.6^{+0.4}_{-0.4}\times10^{56}$	430^{+150}_{-170}	$0.09^{+0.03}_{-0.03}$	179
GW151012	$23.3^{+14.0}_{-5.5}$	$13.6^{+4.1}_{-4.8}$	$15.2^{+2.0}_{-1.1}$	$0.04^{+0.28}_{-0.19}$	$35.7^{+9.9}_{-3.8}$	$0.67^{+0.13}_{-0.11}$	$1.5^{+0.5}_{-0.5}$	$3.2^{+0.8}_{-1.7}\times10^{56}$	1060^{+540}_{-480}	$0.21^{+0.09}_{-0.09}$	1555
GW151226	$13.7^{+8.8}_{-3.2}$	$7.7^{+2.2}_{-2.6}$	$8.9^{+0.3}_{-0.3}$	$0.18^{+0.20}_{-0.12}$	$20.5^{+6.4}_{-1.5}$	$0.74^{+0.07}_{-0.05}$	$1.0^{+0.1}_{-0.2}$	$3.4^{+0.7}_{-1.7}\times10^{56}$	440^{+180}_{-190}	$0.09^{+0.04}_{-0.04}$	1033
GW170104	$31.0^{+7.2}_{-5.6}$	$20.1^{+4.9}_{-4.5}$	$21.5^{+2.1}_{-1.7}$	$-0.04^{+0.17}_{-0.20}$	$49.1^{+5.2}_{-3.9}$	$0.66^{+0.08}_{-0.10}$	$2.2^{+0.5}_{-0.5}$	$3.3^{+0.6}_{-0.9}\times10^{56}$	960^{+430}_{-410}	$0.19^{+0.07}_{-0.08}$	924
GW170608	$10.9^{+5.3}_{-1.7}$	$7.6^{+1.3}_{-2.1}$	$7.9^{+0.2}_{-0.2}$	$0.03^{+0.19}_{-0.07}$	$17.8^{+3.2}_{-0.7}$	$0.69^{+0.04}_{-0.04}$	$0.9^{+0.0}_{-0.1}$	$3.5^{+0.4}_{-1.3}\times10^{56}$	320^{+120}_{-110}	$0.07^{+0.02}_{-0.02}$	396
GW170729	$50.6^{+16.6}_{-10.2}$	$34.3^{+9.1}_{-10.1}$	$35.7^{+6.5}_{-4.7}$	$0.36^{+0.21}_{-0.25}$	$80.3^{+14.6}_{-10.2}$	$0.81^{+0.07}_{-0.13}$	$4.8^{+1.7}_{-1.7}$	$4.2^{+0.9}_{-1.5}\times10^{56}$	2750^{+1350}_{-1320}	$0.48^{+0.19}_{-0.20}$	1033
GW170809	$35.2^{+8.3}_{-6.0}$	$23.8^{+5.2}_{-5.1}$	$25.0^{+2.1}_{-1.6}$	$0.07^{+0.16}_{-0.16}$	$56.4^{+5.2}_{-3.7}$	$0.70^{+0.08}_{-0.09}$	$2.7^{+0.6}_{-0.6}$	$3.5^{+0.6}_{-0.9}\times10^{56}$	990^{+320}_{-380}	$0.20^{+0.05}_{-0.07}$	340
GW170814	$30.7^{+5.7}_{-3.0}$	$25.3^{+2.9}_{-4.1}$	$24.2^{+1.4}_{-1.1}$	$0.07^{+0.12}_{-0.11}$	$53.4^{+3.2}_{-2.4}$	$0.72^{+0.07}_{-0.05}$	$2.7^{+0.4}_{-0.3}$	$3.7^{+0.4}_{-0.5}\times10^{56}$	580^{+160}_{-210}	$0.12^{+0.03}_{-0.04}$	87
GW170817	$1.46^{+0.12}_{-0.10}$	$1.27^{+0.09}_{-0.09}$	$1.186^{+0.001}_{-0.001}$	$0.00^{+0.02}_{-0.01}$	≤ 2.8	≤ 0.89	≥ 0.04	$\geq 0.1\times10^{56}$	40^{+10}_{-10}	$0.01^{+0.00}_{-0.00}$	16
GW170818	$35.5^{+7.5}_{-4.7}$	$26.8^{+4.3}_{-5.2}$	$26.7^{+2.1}_{-1.7}$	$-0.09^{+0.18}_{-0.21}$	$59.8^{+4.8}_{-3.8}$	$0.67^{+0.07}_{-0.08}$	$2.7^{+0.5}_{-0.5}$	$3.4^{+0.5}_{-0.7}\times10^{56}$	1020^{+430}_{-360}	$0.20^{+0.07}_{-0.07}$	39
GW170823	$39.6^{+10.0}_{-6.6}$	$29.4^{+6.3}_{-7.1}$	$29.3^{+4.2}_{-3.2}$	$0.08^{+0.20}_{-0.22}$	$65.6^{+9.4}_{-6.6}$	$0.71^{+0.08}_{-0.10}$	$3.3^{+0.9}_{-0.8}$	$3.6^{+0.6}_{-0.9}\times10^{56}$	1850^{+840}_{-840}	$0.34^{+0.13}_{-0.14}$	1651

>0

LHV

TABLE III. Selected source parameters of the eleven confident detections. We report median values with 90% credible intervals that include

arXiv:1811.12907

Component mass

- $m_1 > m_2$, $q = m_2/m_1$
- many m ~ 30 M_{sun} BHs were observed

arXiv:1811.12907

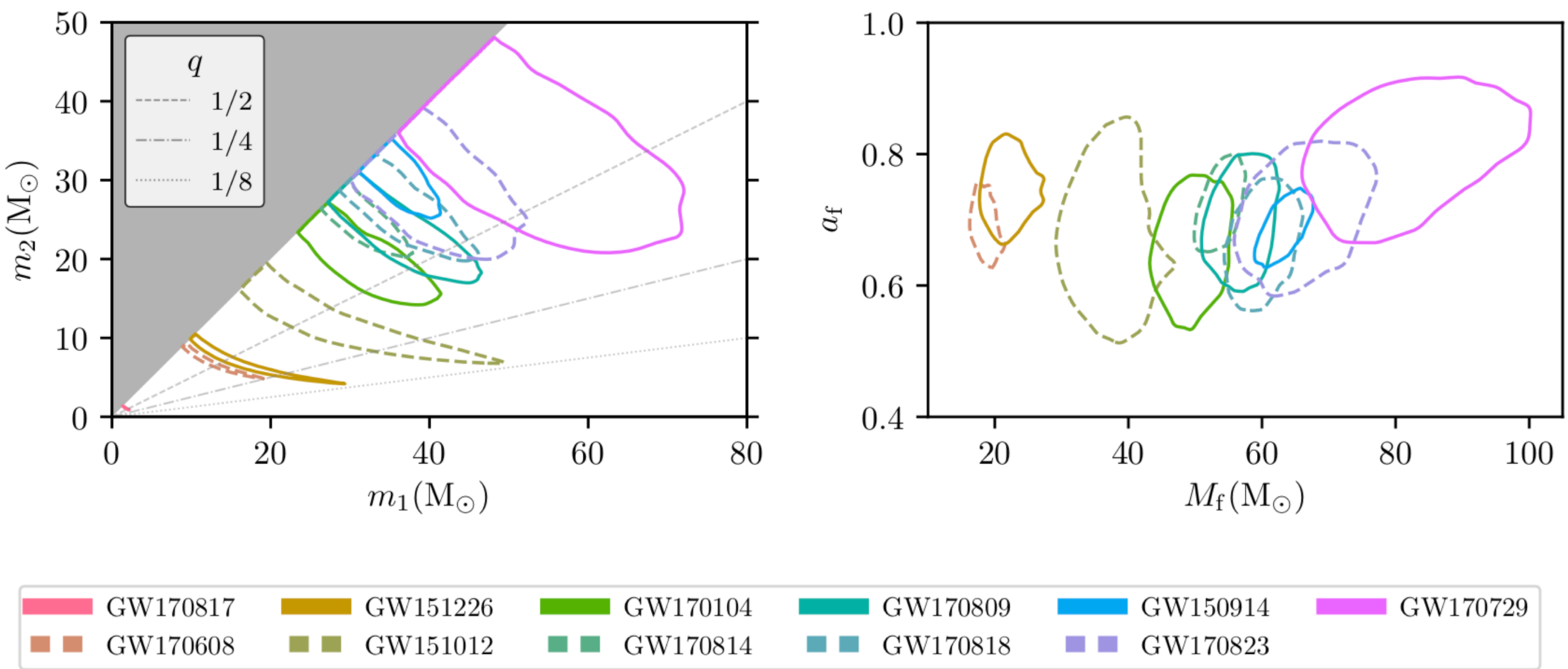

Mass ratio

- $q = m_2/m_1 \sim 1$ is favored

arXiv:1811.12907

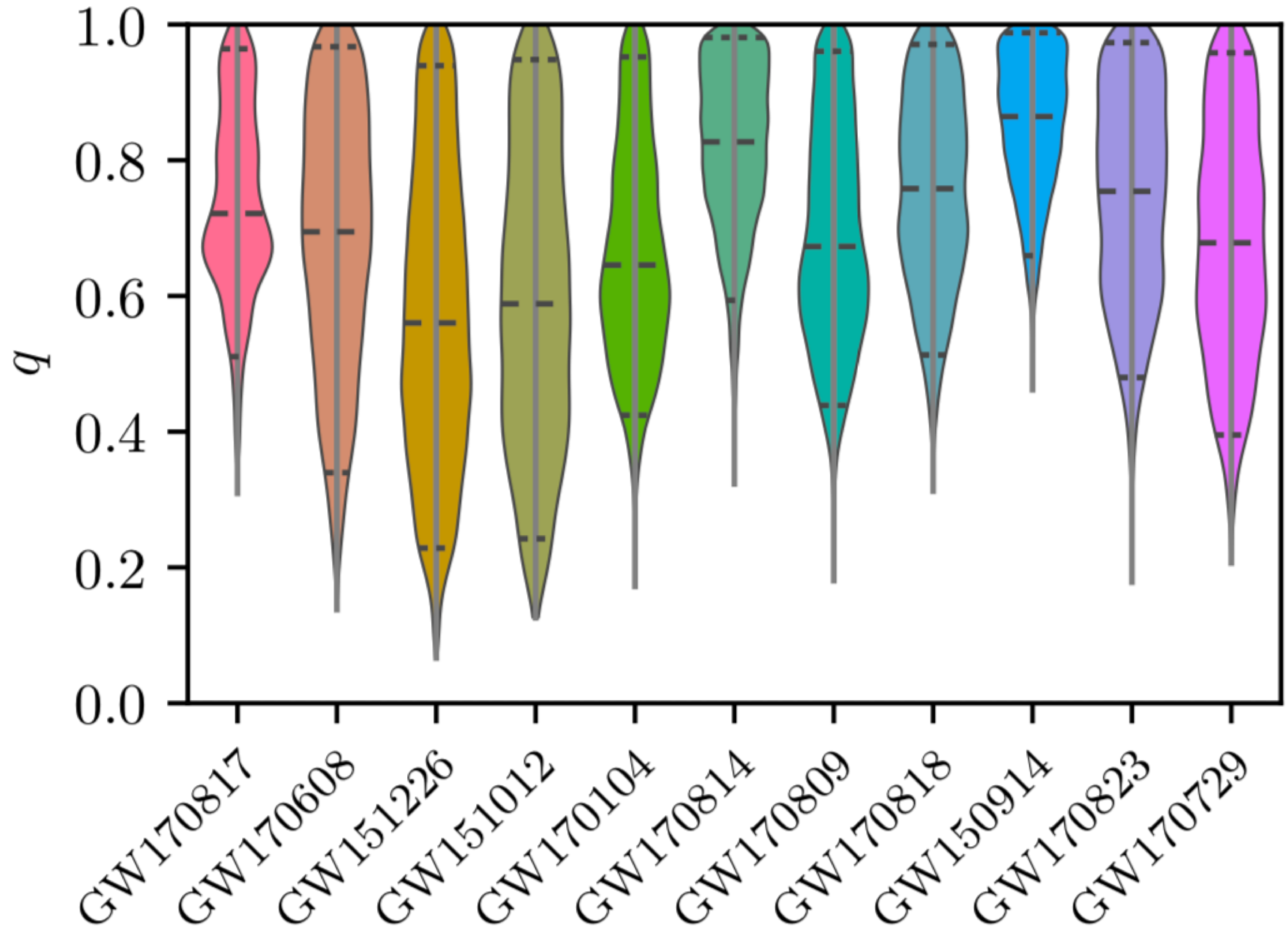

Spin

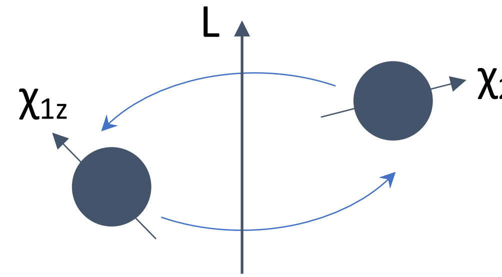

$$\chi_{\text{eff}} = \frac{(m_1\vec{\chi}_1 + m_2\vec{\chi}_2)\cdot\hat{L}_N}{M}$$

- $\chi_{\text{eff}} = 1$: spin is aligned to orbital angular moment
- $\chi_{\text{eff}} = 0$: spin is small or misaligned to orbital angular moment

arXiv:1811.12907

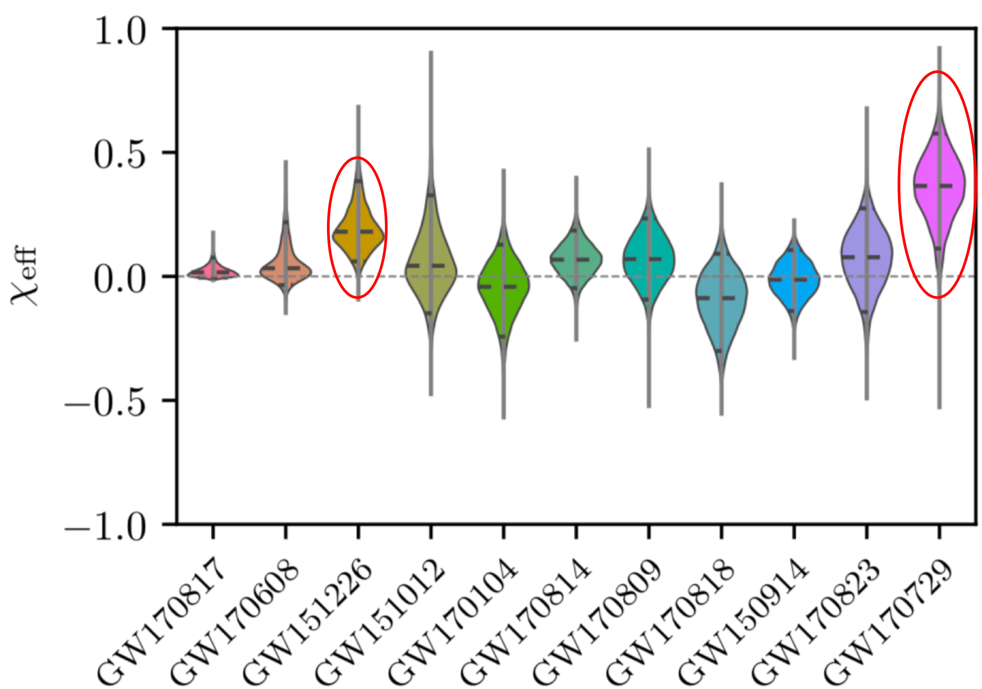

most observed BBHs have χ_{eff} ~ 0
(except for GW151226 & GW170729)

Low spin suggests
"first generation mergers"

Sky localization

- Virgo contributed to three events

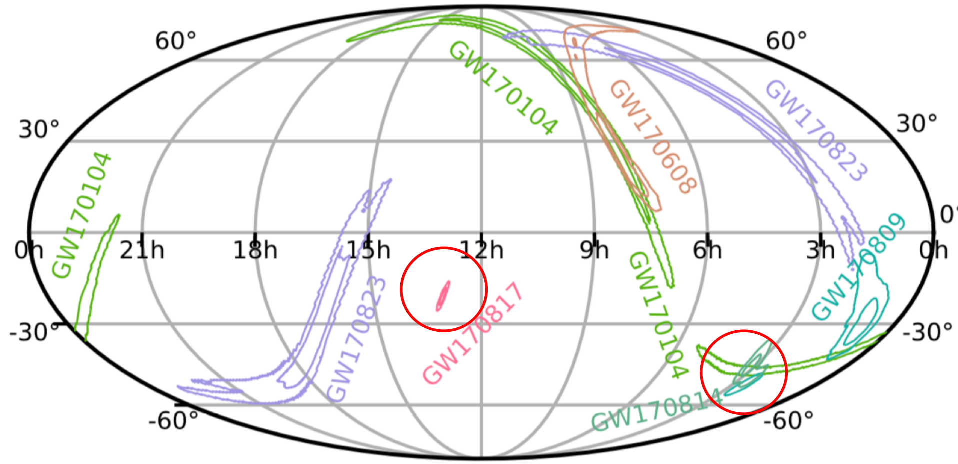

arXiv:1811.12907

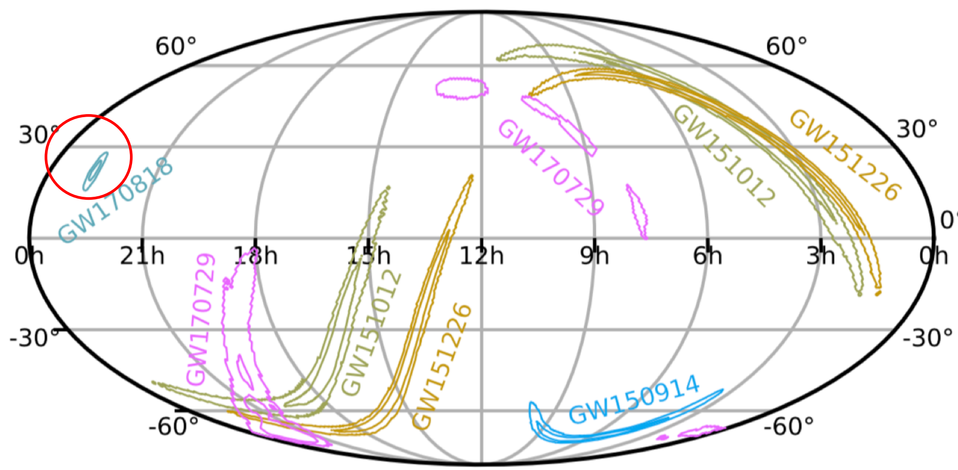

Binary population properties

- is determined by the physical process and evolutionary environments of binaries
  - isolated massive binaries through common envelope
  - dynamical processes in stellar clusters
  - …
- common processes to most pathways
  - mass loss
  - supernova (affected by metalicity)
  - …

- <u>Information on these process can be inferred from the distribution of mass, spin, etc…</u>

Models of mass distribution

- flat-in-log distribution : $p(m_1, m_2) \propto \frac{1}{m_1 m_2}$
- power law : $p(m_1) \propto m_1^{-\alpha}$

- Previous works used these models
- The power law index α was estimated after GW170104, with fixed mass range :

$$m_1 > 5\ M_{sun}\ ,\quad m_1 + m_2 < 100\ M_{sun}$$

$$\Rightarrow \alpha = 2.3^{+1.3}_{-1.4}$$

New (more general) model

- three models (A, B, C) parametrized by

$$p(m_1|\theta) = \Bigg[\underbrace{(1-\lambda_m)A(\theta)m_1^{-\alpha}\Theta(m_{\max}-m_1)}_{\text{power law component}} + \underbrace{\lambda_m B(\theta)\exp\left(-\frac{(m_1-\mu_m)^2}{2\sigma_m^2}\right)}_{\substack{\text{Gaussian component} \\ \text{(only included in model C)}}}\Bigg]\underbrace{S(m_1, m_{\min}, \delta m)}_{\text{low-mass cutoff}}$$

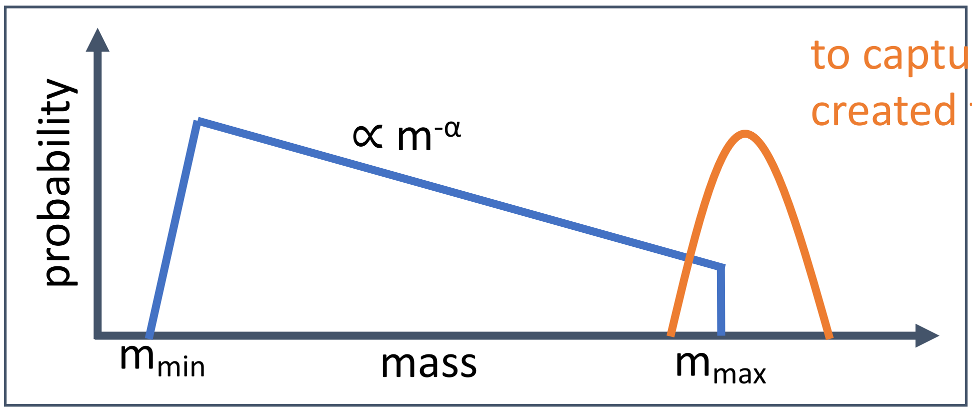

to capture high-mass BHs created from PPISN

arXiv:1811.12940

Model	Mass Parameters								Spin Parameters			
	α	$m_{\max}$	$m_{\min}$	β_q	λ_m	μ_m	σ_m	δm	$\mathbb{E}[a]$	$\mathrm{Var}[a]$	ζ	[illegible]
A	[-4, 12]	[30, 100]	**5**	**0**	**0**	N/A	N/A	N/A	[0, 1]	[0, 0.25]	**1**	[0,
B	[-4, 12]	[30, 100]	[5, 10]	[-4, 12]	**0**	N/A	N/A	N/A	[0, 1]	[0, 0.25]	**1**	[0,
C	[-4, 12]	[30, 100]	[5, 10]	[-4, 12]	[0, 1]	[20, 50]	(0, 10]	[0, 10]	[0, 1]	[0, 0.25]	[0, 1]	[0,

free parameters

Gaussian component : PPISN

- Pulsational Pair Instability SuperNova
  - one of the types of supernova
- remove significant amount of mass from star prior to the core collapse

⇒ mass distribution of born BHs have cutoff

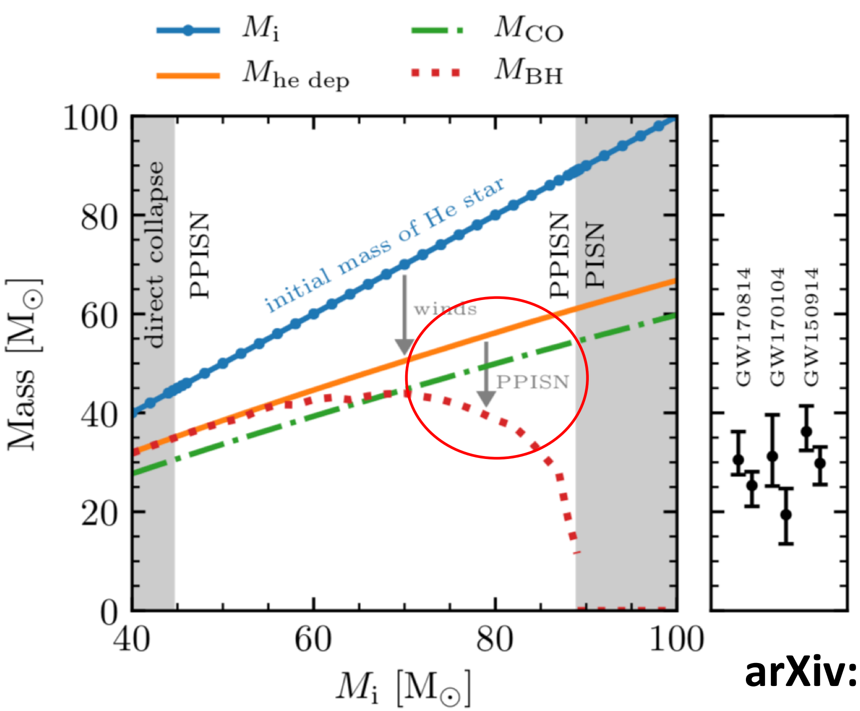

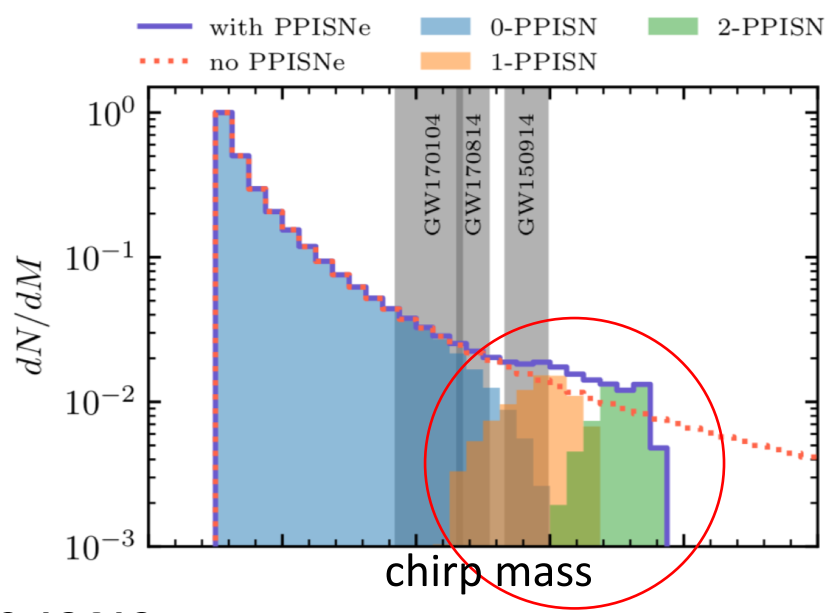

arXiv:1810.13412

Inferred distribution

	α	m_{min} [M_{sun}]	maximum mass (99%)
model A	$0.4^{+1.3}_{-1.9}$	5(fixed)	43.8
model B	$1.6^{+1.5}_{-1.7}$	$7.9^{+1.3}_{-1.9}$	42.8
model C	$7.3^{+4.2}_{-4.6}$	$7.0^{+1.6}_{-1.7}$	41.8

previous assumotion

arXiv:1811.12940

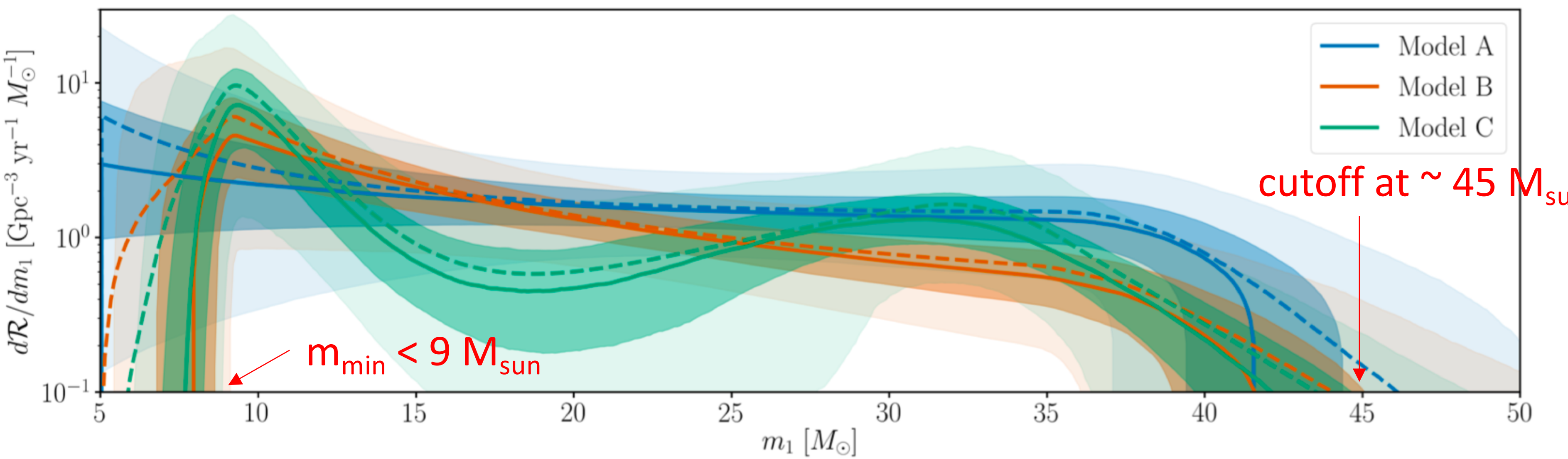

Inferred distribution

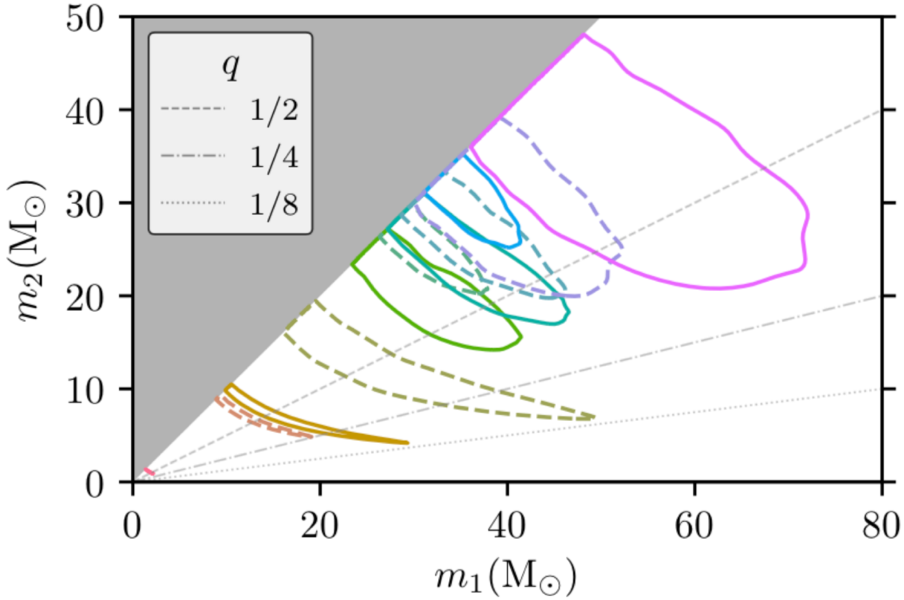

arXiv:1811.12907

arXiv:1811.12940

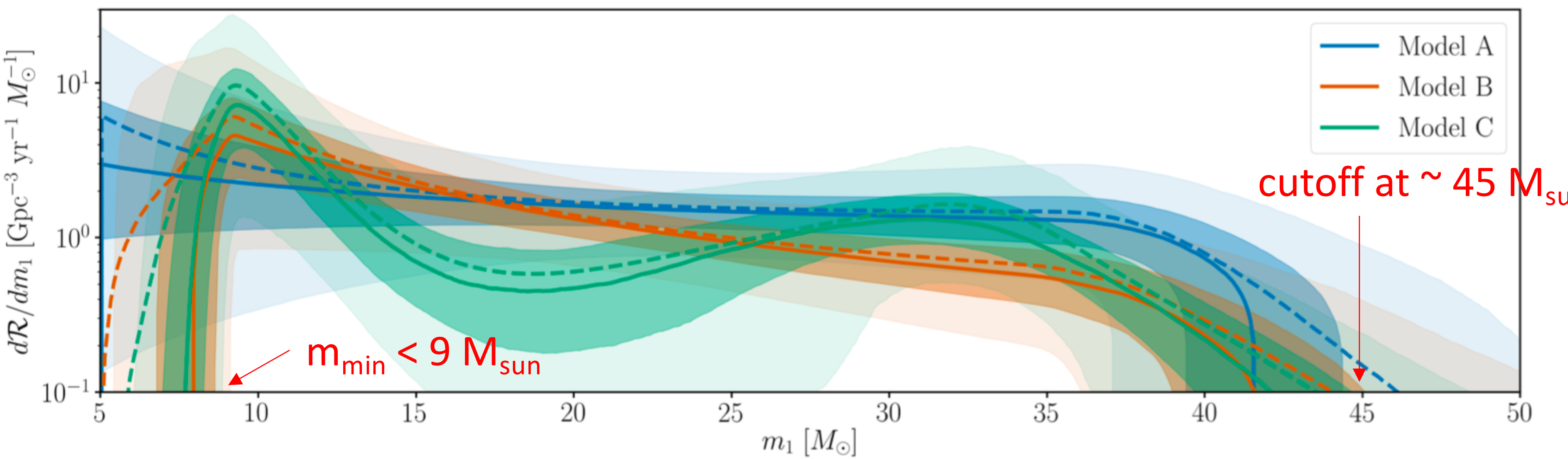

How likely? : Bayesian factor

<u>Bayesian factor</u>

$$\mathrm{BF}^{1}{}_{2} = \frac{\overset{\text{model1}}{p(x|M_1)}}{\underset{\text{model2}}{p(x|M_2)}}$$

(ln BF $^{i}{}_{c}$ >0 : model i is more preferred than model C)

Model	A	B	C, $\lambda_m = 0$	C, $\delta_m = 0$
$\ln \mathrm{BF}^i_C$	-2.37	-1.40	-2.12	0.14

(model A) < (model B) < (model C)

not significant difference

contribution from Gaussian component is likely to exist

Mass gap at 2 - 5 M_{sun}

- suggested by X-ray binary (origin is uncertain)
- BBH distribution cannot confirm this because no BBHs at this mass was observed
  - detectability was not enough

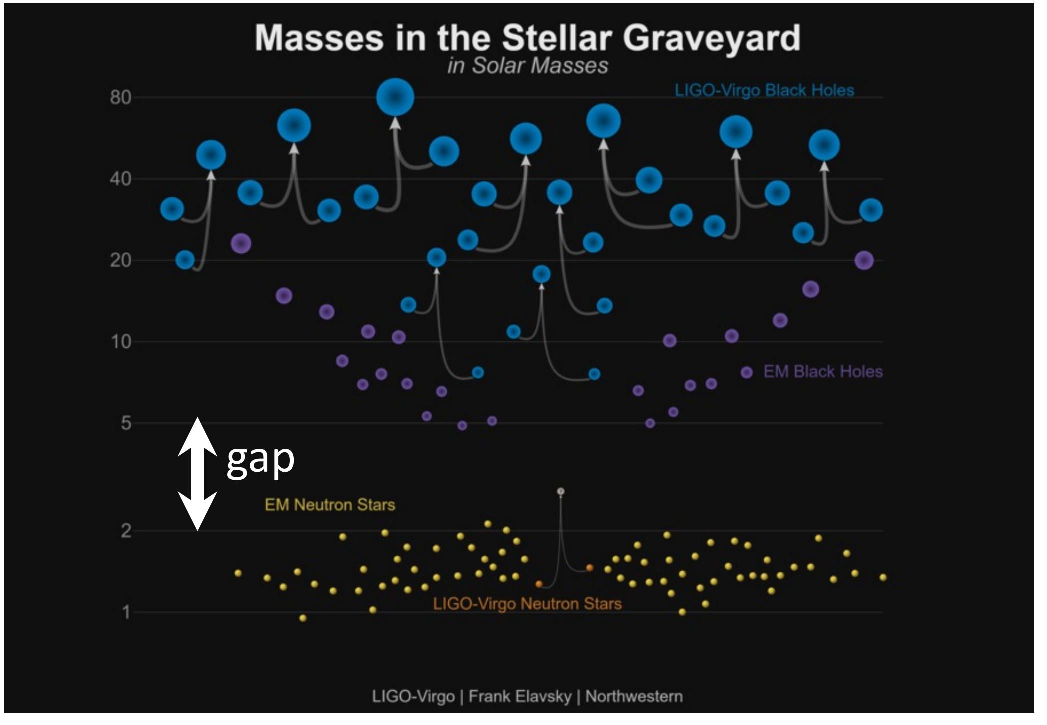

Mass gap above 50 M_{sun}

- The maximum mass of BHs born after PPISN is predicted to be 50 M_{sun}
- BBH mass distribution is consistent with this
  - high-mass cutoff at ~ 45 M_{sun}

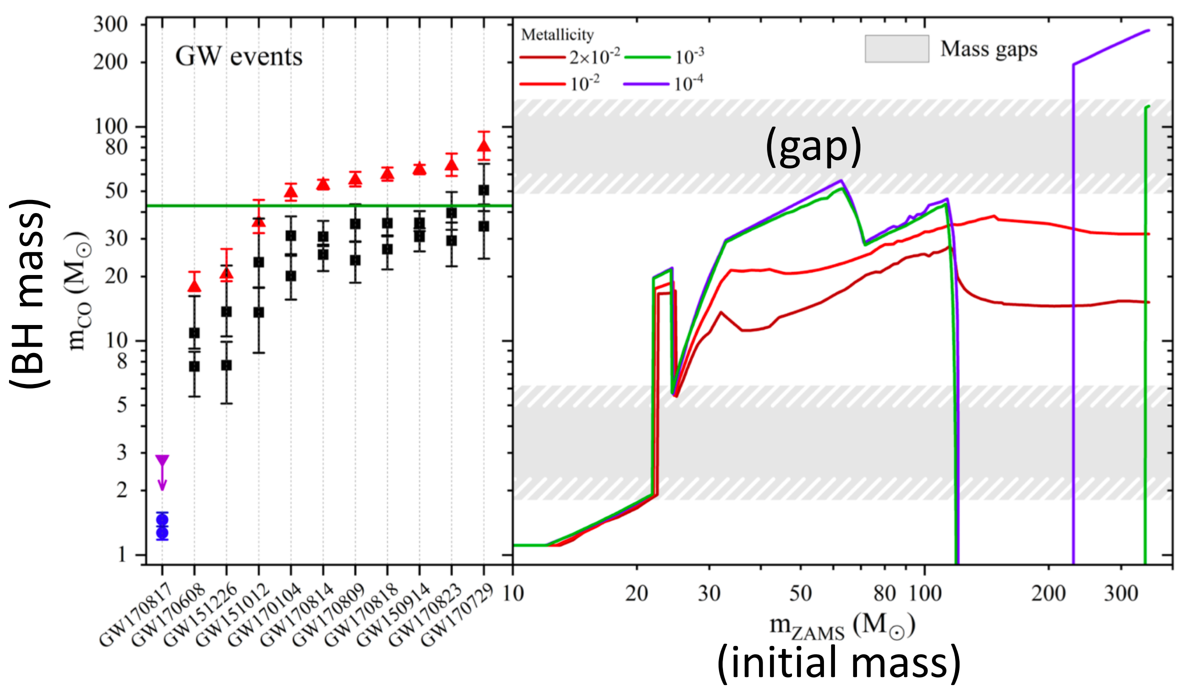

arXiv:1811.12940

Mass ratio

- Model B and C give consistent $\beta > 0$ (95% conf.)
  - large mass ratio (q ~ 0) is disfavored

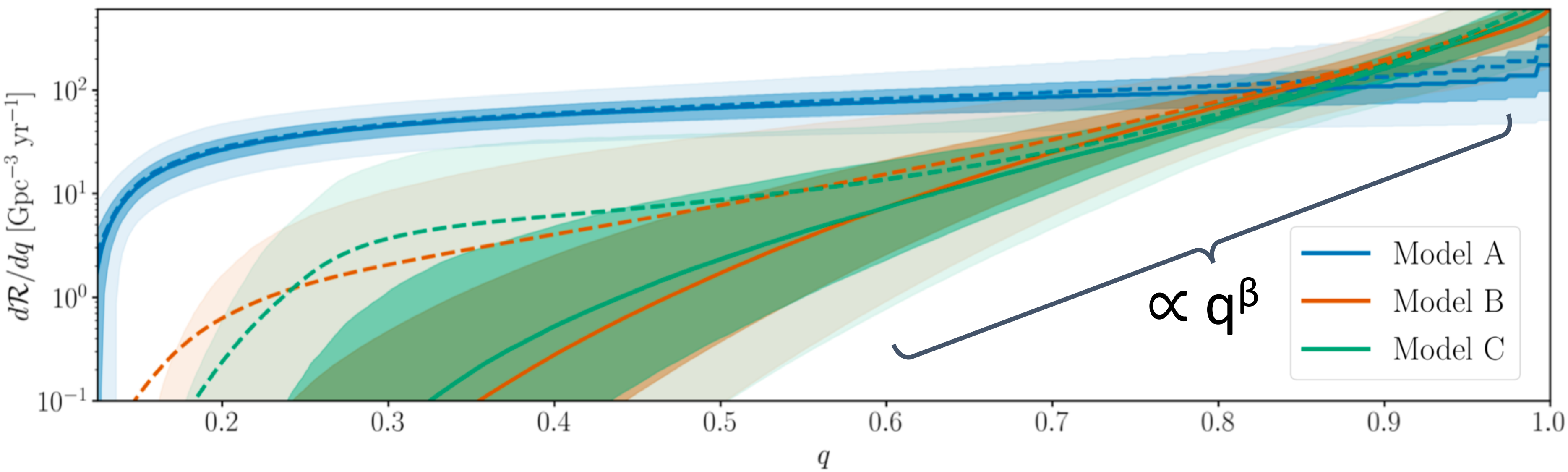

arXiv:1811.12940

Merger rate

- after O1 (3 BBHs) :
  - flat-in-log + power-law

9 - 240 $\mathrm{Gpc}^{-3}\,\mathrm{yr}^{-1}$

Phys. Rev. X 6, 041015

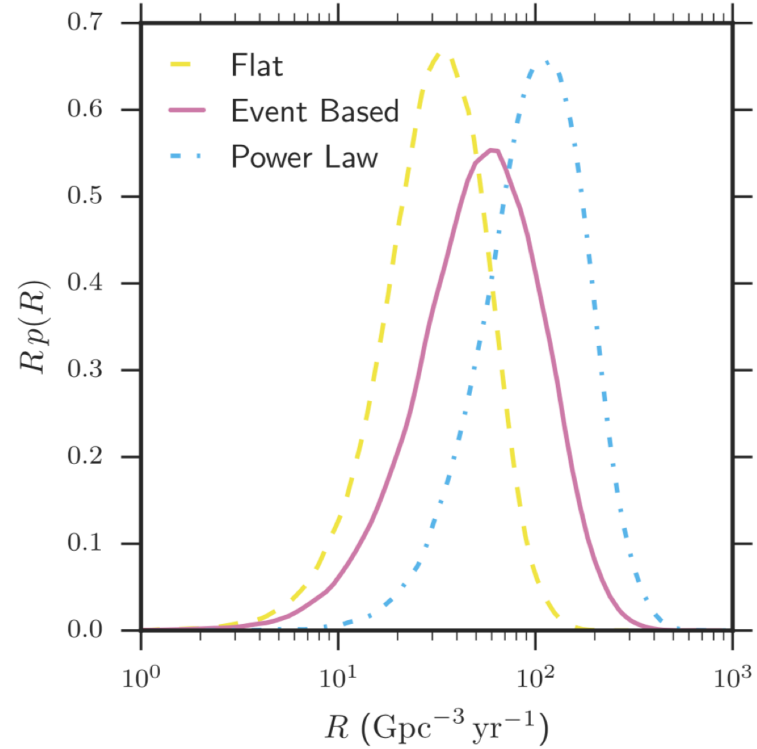

- after O2 (10 BBHs) :
  - model C (power law + Gaussian)

25.9 - 108.5 $\mathrm{Gpc}^{-3}\,\mathrm{yr}^{-1}$

Redshift dependence

$$\boxed{\mathcal{R}(z|\lambda) = \mathcal{R}_0\,(1+z)^{\lambda}}$$

- $\lambda = 0$: uniform merger rate
- $\lambda \sim 3$: (approximately) follows star formation rate

- other factors :
  - metallicity evolution
  - globular cluster formation

- Redshift dependence implies which factors are related?

Evolution of merger rate with z

- $\lambda = 6.5^{+9.1}_{-9.3}$ (using model A with zero spin for simplicity)
  - cannot distinguish different formation rate histories
  - λ > 0 at 88% credibility

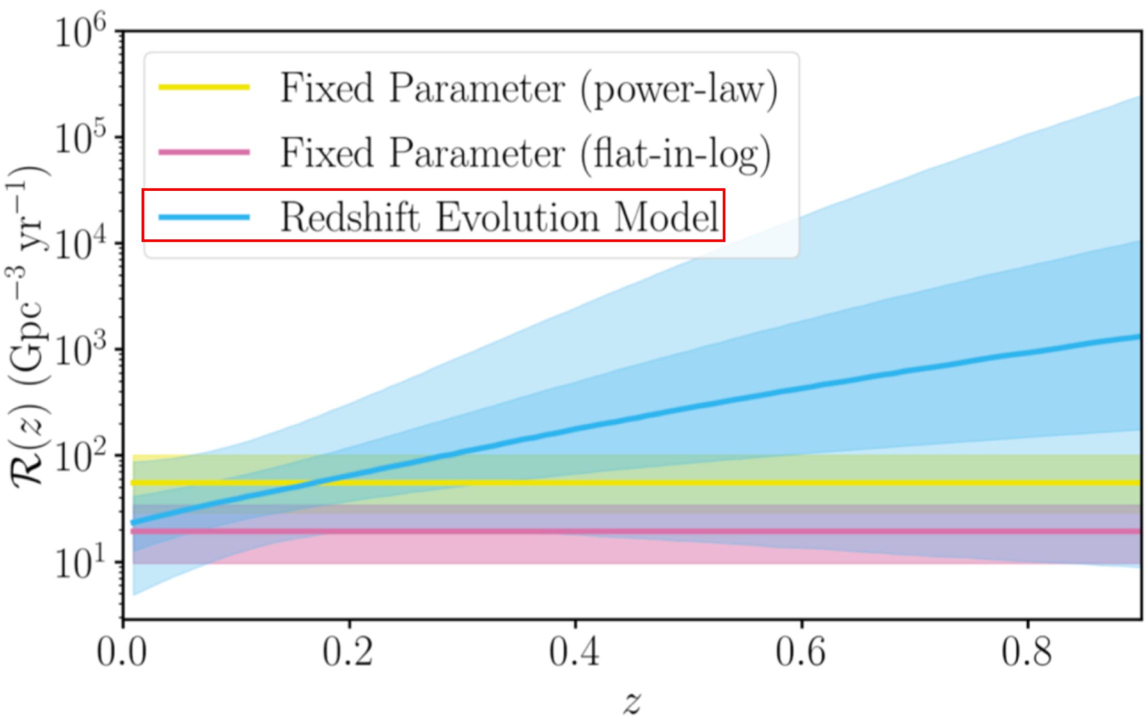

arXiv:1811.12940

Spin magnitude distribution

- large spins are disfavored
  - 50% of BH spins : < 0.27
  - 90% of BH spins : < 0.55

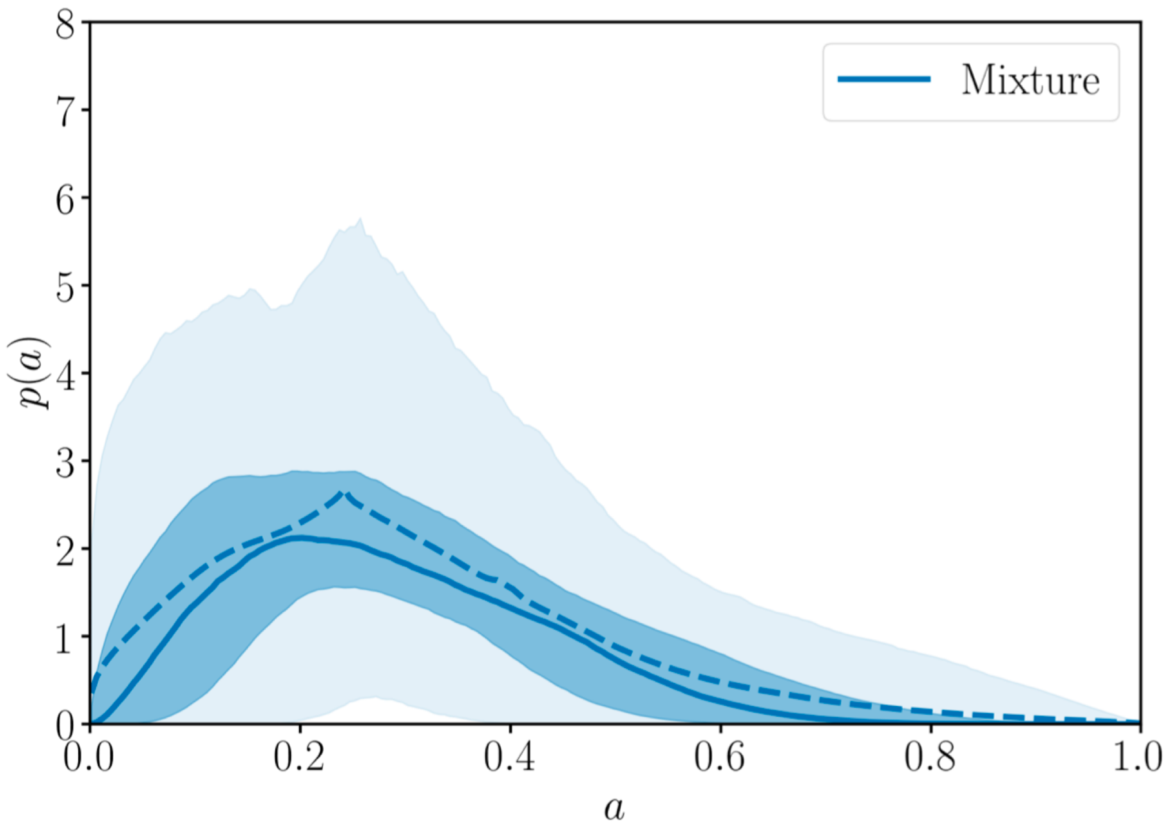

arXiv:1811.12940

Spin tilt distribution

- modeled with parameter ζ as follows

$$p(\cos t_1, \cos t_2 | \sigma_1, \sigma_2, \zeta) = \boxed{\frac{(1-\zeta)}{4}} \text{ isotropic}$$
$$+ \boxed{\frac{2\zeta}{\pi} \prod_{i\in\{1,2\}} \frac{\exp\left(-(1-\cos t_i)^2/(2\sigma_i^2)\right)}{\sigma_i \mathrm{erf}(\sqrt{2}/\sigma_i)}} \text{ Gaussian}$$

ζ = 0 : isotropic
ζ = 1 : Gaussian (aligned)

$\zeta = 0.5^{+0.4}_{-0.5}$

almost no constrain on the
spin orientation distribution is achieved

arXiv:1811.12940

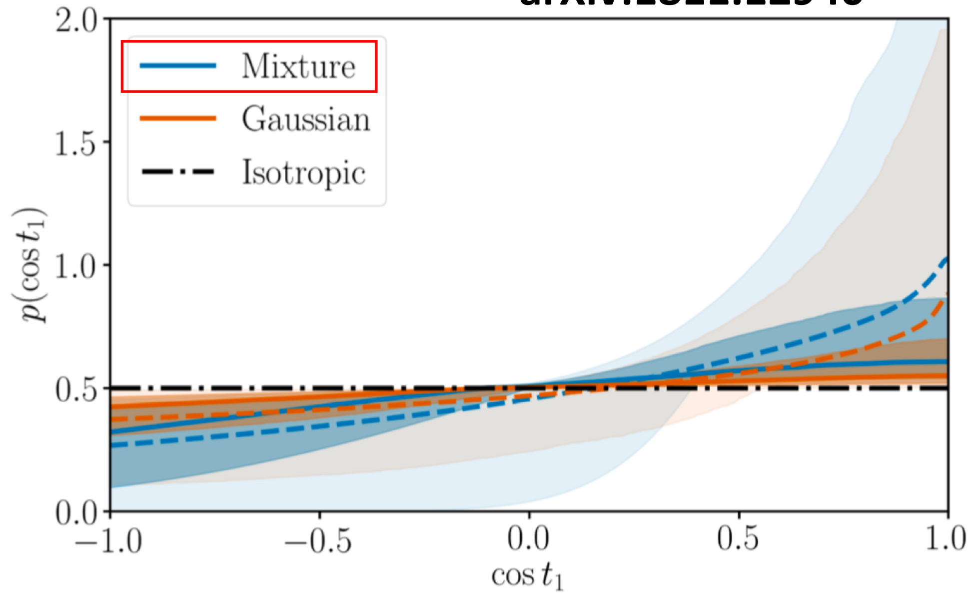

Interpretation of spins

- observation provided only spin <u>magnitude</u> distribution

- spin magnitude is affected by many uncertain processes
  - mass transfer
  - tidal interaction
  - internal mixing
  - …

➢ magnitude distribution is difficult to predict theoretical models

Summary

- Mass distribution :
  - high-mass cutoff at ~ 45 M_{sun} is consistent with PPISN prediction
  - low-mass cutoff at < 9 M_{sun} , but cannot set constrain on the suggested mass gap between 2 M_{sun}(NS) and 5 M_{sun}(BH)
  - large mass ratio is disfavored

- Merger rate :
  - updated : 9 - 240 Gpc^{-3} yr^{-1} (O1) ⇒ 25.9 - 108.5 Gpc^{-3} yr^{-1}
  - increasing with redshift (88% credibility), but the origin cannot be clarified due to large uncertainty

- Spin distribution :
  - large spin magnitude is disfavored (90% of BHs have spins less than 0.55)
  - observation can not provide any preference for orientation distribution
  - due to many uncertain effects, spin magnitude distribution cannot predict theoretical model